Analyzing the Impact of Learning Inputs on Near-to-Far Terrain Traversability Estimation

Ken Ho, Thierry Peynot and Salah Sukkarieh

***Abstract*— With the increasing need to adapt to new environments, data-driven approaches have been developed to estimate terrain traversability by learning the rover's response on the terrain based on experience. Multiple learning inputs are often used to adequately describe the various aspects of terrain traversability. In a complex learning framework, it can be difficult to identify the relevance of each learning input to the resulting estimate. This paper addresses the suitability of each learning input by systematically analyzing the impact of each input on the estimate. Sensitivity Analysis (SA) methods provide a means to measure the contribution of each learning input to the estimate variability. Using a variance-based SA method, we characterize how the prediction changes as one or more of the input changes, and also quantify the prediction uncertainty as attributed from each of the inputs in the framework of dependent inputs. We propose an approach built on Analysis of Variance (ANOVA) decomposition to examine the prediction made in a *near-to-far* learning framework based on multi-task GP regression. We demonstrate the approach by analyzing the impact of driving speed and terrain geometry on the prediction of the rover's attitude and chassis configuration in a Mars-analogue terrain using our prototype rover *Mawson*.**

I. Introduction

For autonomously planetary rovers to explore in challenging environments, estimating terrain traversability is necessary to anticipate situations that may compromise its safety and ability to conduct exploration missions, since many scientifically interesting sites on Mars are located in rough and heterogeneous terrain that poses significant risks to the rover [1]. As the Rover-Terrain Interaction (RTI) in such terrain can be very difficult to model correctly, data-driven approaches have been developed to estimate terrain traversability by learning the rover's response on the terrain based on experience. [2] proposed a framework to estimate the mechanical properties of the terrain using proprioceptive data collected from experiments. A terramechanics model was then used to predict the rover's wheel slip on the terrain.

Recent literature showed that the rover's response on the upcoming terrain can be predicted by learning the correlation between exteroceptive and proprioceptive sensor information [3]. This concept is known as *near-to-far* learning. [4] extended the work in [2] by first using proprioceptive training data to learn terrain parameters, and then associated the parameters with terrain classes from a vision-based classifier to anticipate vehicle slip in operation. Similar frameworks to associate mechanical terrain properties with exteroceptive information include [5], which predicted soil softness using the learnt associations between angular acceleration along the pitch and roll axes and color descriptors. By learning the association between terrain appearance and RTI during experiments, these approaches are able to anticipate situations that are hazardous to the rover.

The aforementioned approaches commonly use multiple learning inputs to adequately describe the various aspects that are correlated with terrain traversability. These correlations are learnt using complex learning algorithms often considered as "black box" functions that provide little or no information about the impact of each learning input on the resulting estimate. Without a systematic procedure to determine the relevance of the learning inputs, it is difficult to understand the shortcomings of the system, or to evaluate the suitability of new learning inputs. The overall accuracy of the estimator and the validity of the error can be checked using cross validation [7]. However, in order to better understand the effects of the learning inputs, we need to analyze the contribution or impact of the inputs on the estimate.

Sensitivity analysis methods can be used to better understand the responses of estimation systems [8]. The Sobel index [9], based on variance decomposition, measures sensitivity by expanding the global variance into partial variances. To validate the response of Gaussian Process (GP) regression, frameworks based on sensitivity analysis methods were proposed in [10], [11]. These frameworks analyzed the effects of input variables on the estimate. However, both of the above methods rely on the assumption that the input variables are independent. If the input variables are dependent, the amount of response variance may be influenced by its dependence on other inputs, and thus lead to incorrect interpretations [12].

To account for the contribution from dependent inputs, [13] proposed to decompose the partial variance of an input into a correlated and an uncorrelated contribution components, assuming a linear effect from each component on the response. This approach was later extended by approximating the effect using a sum of functional components of low dimensions, and then computing the decomposition of response variance as a sum of partial variances [14]. [15] proposed sensitivity analysis methods to account for non-constant (heteroscedastic) variances in the estimate.

In this paper we analyze the impact of learning inputs on a near-to-far terrain traversability estimate using a sensitivity analysis method built on Analysis of Variance (ANOVA)

The work was partly supported by the Australian Centre for Field Robotics (ACFR) and the NSW government.

K. Ho, T. Peynot and S. Sukkarieh are with the Australian Centre for Field Robotics, University of Sydney, NSW 2006, Australia, (k.ho,tpeynot,salah)@acfr.usyd.edu.au. T. Peynot is also with the School of Electrical Engineering and Computer Science, Queensland University of Technology, Brisbane, Australia, t.peynot@qut.edu.au.

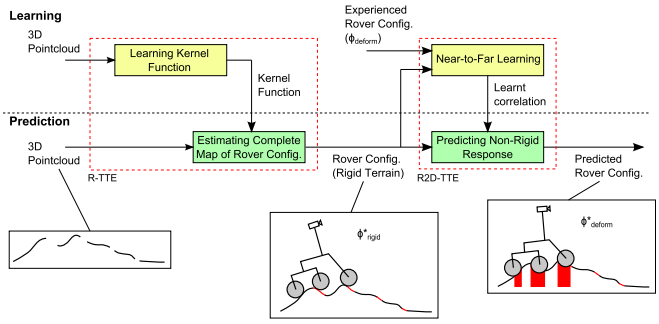

Fig. 1. System architecture of our approach for terrain traversability estimation. Given an incomplete point cloud, R-TTE makes a continuous initial estimate of the rover configuration over the entire map, assuming the terrain is rigid. R2D-TTE then refines this estimate to account for possible terrain deformation.

decomposition in a framework of dependent inputs. This quantifies the contributions from each learning input to the variability of the resulting estimate, including the extent at which the estimate uncertainty can be attributed to the learning inputs. The method first decomposes the estimate into a multi-dimensional representation of primary and interaction effects between the learning inputs. The analytical sensitivity measure is then calculated for combinations of learning inputs, and indicates the significance of each learning input. We validate the approach with experimental data collected using a prototype rover on a Mars-analogue terrain.

The paper is organized as follows. Sec. II outlines our near-to-far learning framework previously proposed in [16] to compute an estimate of the rover attitude and configuration that accounts for the effects of terrain deformation. Sec. III details the theory and implementation of sensitivity analysis method to decompose the resulting estimate. In Sec. IV and V we describe the experimental validation of the approach and discuss the results obtained, including the impact of driving speeds and terrain geometry on the resulting estimate. Finally, Sec. VI proposes a conclusion and possible future work.

II. Estimating Traversability in Partially Occluded and Deformable Terrain

We proposed a framework in [17] and [16] to address the problems of incomplete terrain data and terrain deformation sequentially in separate components. The proposed system architecture can be seen in Fig. 1. Given incomplete terrain data, the first component, named *Rigid-Terrain Traversability Estimation* (R-TTE), provides an initial estimate of the rover configuration Φ^*_{rigid} *before* any terrain deformation may occur. This is equivalent to assuming that the terrain is rigid. The second component, *Rigid-to-Deformable Traversability Estimate* (R2D-TTE), then refines this prediction by accounting for the effects of terrain deformation on rover configuration, learnt from experience. We name this final estimate Φ^*_{deform}. To account for uncertainties in the observations and knowledge base, both processes are stochastic.

A. R-TTE

The R-TTE module within the framework addresses the problem of incomplete terrain data. Using the method we proposed [17], we estimate a complete map of Φ^*_{rigid} by performing GP regression over an incomplete map of rover configuration. This approach exploits the explicit correlation in rover configuration during operation by learning a kernel function from experience. We set up the traversability estimation scenario as a GP regression problem to predict $\Phi^*_{rigid}(x, y, \psi)$ at each position (x, y) on a Digital Elevation Map (DEM) over different heading angles ψ. The GP posterior (estimate) $\bar{f}^*$ and covariance $cov(f^*)$ can be given as:

$$\bar{f}^* = K(X^*, X)[K(X, X) + \sigma_n^2 I]^{-1} z \tag{1}$$

$$cov(f^*) = K(X^*, X^*) - K(X^*, X)[K(X, X) + \sigma_n^2 I]^{-1} K(X, X^*) \tag{2}$$

where K represents the covariance matrix evaluated using the learnt kernel function at all the pairs of training points X and query points X^*, σ_n is the noise variance, and z is the training target.

B. R2D-TTE

The R2D-TTE module, previously proposed by the authors in [16], refines the estimate provided by R-TTE by accounting for the effects of terrain deformation. We extended the estimation process to exploit the local variations in Φ_{rigid} that correlate with the actual rover configuration resulting from terrain deformation, i.e. Φ_{deform}, and include driving speed as an additional learning input. This idea is implemented in a near-to-far learning approach by learning the correlation between the initial prediction, Φ^*_{rigid}, its local variations, and experience in Φ_{deform} collected during training (Fig. 1). Fig. 2 illustrates the outline of the R2D-TTE approach. During learning, the rover observes a patch of terrain and predicts Φ^*_{rigid}. When the rover traverses over the patch of terrain, it learns the correlation between Φ^*_{rigid} and the experienced rover configuration Φ_{deform} with terrain deformation. Once the training is complete, in operation, the rover uses the learnt correlations to predict Φ^*_{deform} from new exteroceptive data.

Learning is performed in a multi-task heteroscadastic GP framework that considers the interaction between multiple training inputs and targets. We use multiple-input GP regression by Automatic Relevance Determination (ARD) to learn the correlation between the training inputs X and each component in the target z. Using a separate lengthscale for each component in the training input, ARD determines the orders of interaction that are important in the GP regression [18]. We use convolution processes to account for the correlations between estimation outputs [19]. This approach uses a convolution between a smoothing kernel k_q and latent functions $u(z)$ to express each output f_q:

$$f_q(X) = \int_{-\infty}^{\infty} k_q(X - z)\, u(z) dz \tag{3}$$

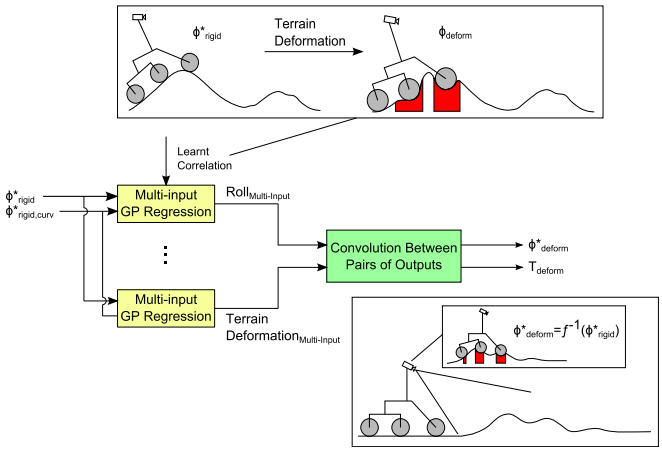

Fig. 2. Illustration R2D-TTE process to account for the effects of terrain deformation on the rover configuration, using correlations learnt in experiments.

We then use multiplication of Gaussian distributions to determine the correlation between pairs of outputs as well as between any given output and the latent function:

$$cov\left[f_q(X), f_s(X')\right] = \sum_{r=1}^{R} \int_{-\infty}^{\infty} k_{qr}\left(X - z\right) \int_{-\infty}^{\infty} k_{sr}\left(X' - z'\right) k_{u_r u_r}\left(z, z'\right) dz' dz,$$
$$cov\left[f_q(X), u_r(z)\right] = \int_{-\infty}^{\infty} k_{qr}\left(X - z'\right) k_{u_r u_r}\left(z', z\right) dz'. \tag{4}$$

Using the covariance matrices in Eqs. (4), we perform joint-prediction of the estimation outputs by iteratively calculating the matrices for each latent function and output.

III. Sensitivity Analysis

We use Analysis of Variance (ANOVA) decomposition to analyze the effects of learning inputs on the resulting estimate. This method decomposes the total mean and variance of the GP estimator into contributions from dependent inputs. The percentage of total contribution attributed among the inputs then provides a measure of importance of the interaction effect between each learning input and the resulting estimate [15].

To decompose the resulting estimate, we need to first find the marginal effect $\bar{y}_e(x_e)$. This is the overall effect of all variables x_e on the estimate, and is defined by integrating out all other variables [10]:

$$\bar{y}_e(x_e) = \int_{\otimes_{j \notin e} \mathcal{X}_j} y(x_e, x_{-e}) \prod_{j \notin e} w_j(x_j) dx_j \quad \text{for } x_e \in \otimes_{j \in e} \mathcal{X}_j, \tag{5}$$

where $w_j(x_j)$ is a weight function that represents interest among x_j, and $\mathcal{X}_j$ denotes the values of interest for variable x_j.

We then use Eq. (5) to decompose the resulting estimate $y(x)$ into corrected effects involving the contributions from any number of variables $x \in \mathcal{X}$:

$$y(x) = \mu_0 + \sum_{j=1}^{d} \mu_j(x_j) + \sum_{j=1}^{d-1} \sum_{j'=j+1}^{d} \mu_{jj'}(x_j, x_{j'}) + \ldots + \mu_{1\ldots d}(x_1, \ldots, x_d), \tag{6}$$

where μ_0, $\mu_j(x_j)$, $\mu_{jj'}(x_j, x_{j'})$ are the overall average, corrected primary effect, and corrected interaction effect respectively:

$$\begin{aligned} \mu_0 &= \int_{\mathcal{X}} y(x) w(x) dx \\ \mu_j(x_j) &= \bar{y}_j(x_j) - \mu_0 \qquad \text{for } x_j \in \mathcal{X}_j \\ \mu_{jj'}(x_j, x_{j'}) &= \bar{y}_{jj'}(x_j, x_{j'}) - \mu_j(x_j) - \mu_{j'}(x_{j'}) - \mu_0 \\ &\qquad \text{for } x_j, x_{j'} \in \mathcal{X}_j \otimes \mathcal{X}_{j'} \end{aligned} \tag{7}$$

where x_j is a complementary set of $x_{j'}$.

For example, to examine the contributions from learning inputs x_1 and x_2 on the resulting estimate, we can consider the overall joint effect:

$$\bar{y}_{12}(x_1, x_2) = \mu_0 + \mu_1(x_1) + \mu_2(x_2) + \mu_{12}(x_1, x_2) \quad \text{for } x_1, x_2 \in \mathcal{X}_1 \otimes \mathcal{X}_2 \tag{8}$$

In practice, we first estimate the marginal effects using a best linear unbiased predictor (BLUP) [10], and then compute the corresponding estimated corrected effect by subtracting all estimated lower-order corrected effects. Using this decomposition, we can determine the impact of the learning inputs on the resulting estimate as a function of its interaction with other learning inputs.

The variance of the estimate can also be decomposed as [14]:

$$V(y(x)) = \sum_{u \in S} \left[V(f_j(x_j)) + Cov(f_j(x_j), f_{j'}(x_{j'}))\right] \tag{9}$$

where $f_{j'}(x_{j'}) = f(x) - f_j(x_j)$.

To quantify the contribution of the overall learning input x_j to the resulting estimate, we calculate the analytical sensitivity measure S_j that accounts for both the estimate mean and uncertainty, which can be computed as [20]:

$$S_j = \frac{V[\mu_j(x_j)] + Cov[\mu_j(x_j), \mu_{j'}(x_{j'})]}{V[y(x)]} \tag{10}$$

In our implementation, we compute S_j for each learning input to determine their impact on the resulting GP regression estimate.

IV. Experimental Setup

A. Platform - Mawson Rover

The experiments were conducted using *Mawson*, a 6-wheeled prototype rover platform with a rocker-bogie chassis and individual steering motors on each wheel (see Fig. 3(a)). Mawson is approximately $80cm$ long, $63cm$ wide,

and $90cm$ tall. The radius of each wheel is $5cm$. Onboard sensors include:

- two color cameras and a RGB-D camera (Microsoft Kinect^{TM}) mounted on a pan-tilt unit, tilted down $\approx 20^{\circ}$, used primarily for terrain modeling,
- two Hall-effect encoders measuring the two rear bogie angles (α_1, α_2 in Fig. 3(b)), and a potentiometer on the rocker differential,
- an Intersense^{TM} IS-1200 motion capture system that fuses data from a visual camera and an inertial measurement unit to provide the 6-DOF sensor pose.

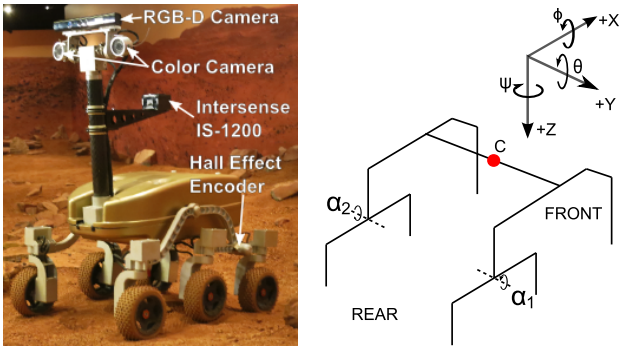

(a) Mawson rover (b) Chassis configuration

Fig. 3. Experimental rover platform.

In our experiments, the Intersense IS-1200 unit provided localization of the rover with respect to a constellation of fiducials in the environment that were geo-referenced using surveying equipment, with an average accuracy of $2cm$ in position and 1° in rotation. Since the experiments were performed in an indoor environment, we used the RGB-D camera to obtain 3D point clouds of the terrain. For outdoor operations, where the RGB-D camera may be unable to provide reliable data, dense stereovision can be used instead without affecting the conclusions of this study. In order to associate the acquired point clouds with the localization of the rover, we performed exteroceptive calibration between the two sensors off-line using the method in [21].

B. Test Environment

We conducted our experiments at the Marsyard, a Mars-analogue terrain in Sydney, Australia (see Fig. 4). The Marsyard is approximately $15m \times 8m$ and contains slopes, soil and rocks similar to Martian terrain. The typical obstacle size in the Marsyard is approximately $0.05m$ to $0.2m$ in radius. Combined with the mixed sizes in gravel granules, this presents a considerable challenge in traversability for Mawson since its wheel radius is $0.05m$.

C. Experimental Data For Learning

We performed a range of traversals over different terrain to engage Mawson in a variety of situations that it is likely to encounter during operation. Before the rover traversed on the terrain, we recorded the point cloud of the terrain using an external depth sensor (Asus Xtion^{TM}). As the rover traversed the terrain, we collected the experienced rover configuration Φ_{deform} using the Intersense sensor, as well as terrain data using the onboard depth sensor. After terrain traversal, we acquired another pointcloud of the terrain using the external depth sensor. To quantify terrain deformation from terrain traversals, we compared the DEM generated from the point cloud of the terrain before and after rover traversal. In order to obtain terrain geometry data in the same navigation frame used by Mawson for its localization, we first used a theodolite to find the transformation between a reference point on Xtion sensor and the navigation frame of the rover [21]. Nearest-Neighbor Iterative Closest Point was then used to find the transformation between the reference point and the image frame.

Fig. 4. Marsyard in Sydney, Australia.

D. GP Learning Inputs and Outputs

The training input X of our GP includes $\Phi^{*}_{rigid}(s)$, as defined in Fig. 3(b), and its local curvatures:

$$X = [\phi, \phi_{curv}, \theta, \theta_{curv}, \alpha_1, \alpha_{1_{curv}}, \alpha_2, \alpha_{2_{curv}}]. \quad (11)$$

The training target z includes the actual rover configuration $\Phi_{deform}(s)$ and terrain deformation $\mathcal{T}_{deform}$. We define $\mathcal{T}_{deform}$ as the combined planform and platform curvature of the rover configuration on deformed terrain:

$$z = [\Phi_{deform}, \mathcal{T}_{deform}], \quad (12)$$

$$\Phi_{deform} = [\phi_{deform}, \theta_{deform}, \alpha_{1_{deform}} \alpha_{2_{deform}}], \quad (13)$$

$$\mathcal{T}_{deform} = [\phi_{curv}, \theta_{curv}, \alpha_{1_{curv}}, \alpha_{2_{curv}}]_{deform}. \quad (14)$$

The GP training data was discretized over 8 equally spaced yaw angles to facilitate learning with fewer data points.

V. Experimental Validation

A. Predicting Φ_{deform} using R2D-TTE

The experimental validation was performed using data collected from a $30m$ drive on the Marsyard. Figure 5 illustrates the rover configuration estimated between 12 and $22m$ along its traveled distance using R-TTE and R2D-TTE, with the rover operating at different speeds. Using correlations between exteroception, driving speed, and actual rover experience, the estimation made using R2D-TTE is able to anticipate the effects of terrain deformation.

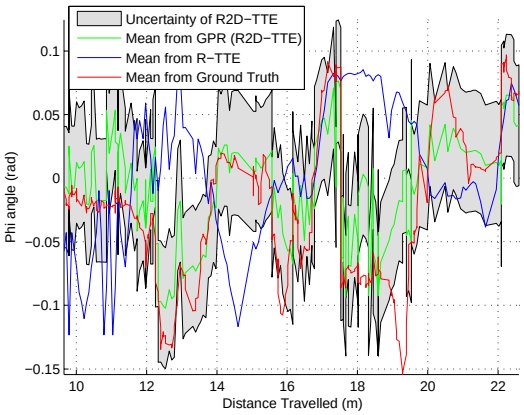

(a)

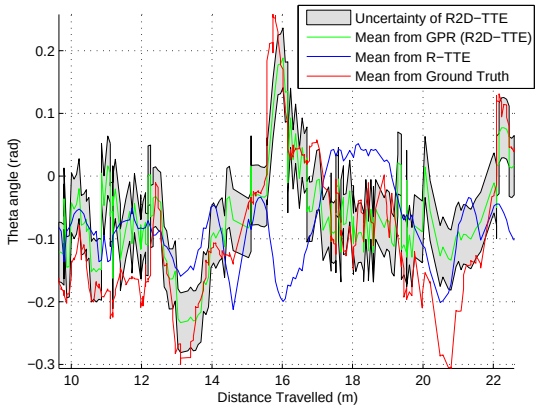

(b)

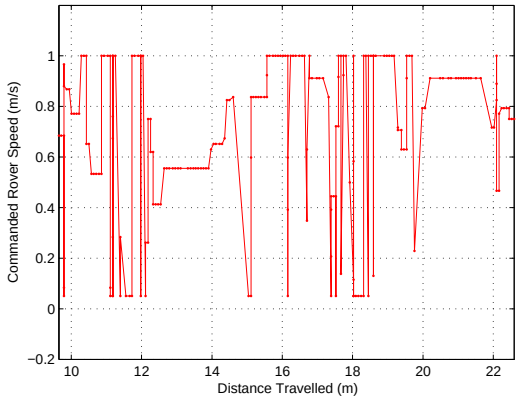

(c)

Fig. 5. GP regression results for predicting roll ϕ (a) and pitch θ (b). The commanded speed of the rover is shown in (c). The improvement in accuracy using R2D-TTE (green) over R-TTE (blue) can be seen particularly between 14 and $20m$ along its traveled distance where there is significant terrain deformation.

B. Sensitivity Analysis of Φ^*_{deform}

1) Analytical Sensitivity Measure: Table I shows the analytical sensitivity measure of first-order effects from each learning input to Φ_{deform}. It can be seen that Φ_{rigid} in the learning inputs contributes to the highest values in first order effects in Φ_{deform} (highlighted in Table I). This is because Φ_{rigid} is expected to be very similar to Φ_{deform} in areas with minimal terrain deformation.

TABLE I

ANALYTICAL SENSITIVITY MEASURE OF FIRST ORDER EFFECTS FROM EACH LEARNING INPUT TO Φ_{deform}.

	ϕ_{deform}	θ_{deform}	$q1_{deform}$	$q2_{deform}$
ϕ_{rigid}	0.12	0.08	0.04	0.04
θ_{rigid}	0.10	0.13	0.06	0.07
$q1_{rigid}$	0.04	0.01	0.07	0.04
$q2_{rigid}$	0.03	0.05	0.03	0.08
$\phi_{rigid,curv}$	0.04	0.06	0.01	0.02
$\theta_{rigid,curv}$	0.02	0.01	0.02	0.01
$q1_{rigid,curv}$	0.01	0.03	0.05	0.02
$q2_{rigid,curv}$	0.03	0.01	0.04	0.04
$speed$	0.05	0.04	0.02	0.03
$\sum_{primary}$	0.44	0.41	0.34	0.35

Table II shows the analytical sensitivity measure of selected interaction effects from combinations of learning inputs to Φ_{deform}. The interaction effects with the highest impact on the estimated rover roll and pitch are highlighted, and the sum of the selected interaction effects is shown at the bottom of the table. It can be seen that the interaction effects from combinations of Φ_{rigid} and driving speed are the highest compared to other combinations of learning inputs. This validates the choice of adding driving speed as a learning input. The interaction effects of $\Phi_{rigid,curv.}$ with other learning inputs are also significant, having an analytical sensitivity measure between 50 and 65% of the highest values in the estimate of ϕ_{deform} and θ_{deform}.

It should be noted that other combinations of interaction effects also contribute to the resulting estimate Φ_{deform}, but are minor and thus not shown in Table II for clarity.

TABLE II

ANALYTICAL SENSITIVITY MEASURE OF SELECTED INTERACTION EFFECTS FROM EACH LEARNING INPUT TO ϕ_{deform} AND θ_{deform}.

	ϕ_{deform}	θ_{deform}
$(\phi,\theta)_{rigid}$	0.05	0.04
$(\phi,q_1)_{rigid}$	0.03	0.04
$(\phi,q_2)_{rigid}$	0.03	0.02
$(\theta,q_1)_{rigid}$	0.02	0.01
$(\theta,q_2)_{rigid}$	0.03	0.02
$(\phi,\theta,q_1)_{rigid}$	0.06	0.03
$(\phi,\theta,q_2)_{rigid}$	0.05	0.03
$(\phi,\theta,\phi_{curv})_{rigid}$	0.04	0.02
$(\theta,q_1,\theta_{curv})_{rigid}$	0.03	0.02
$(\phi,\theta)_{rigid},speed$	0.03	0.04
$\sum_{interaction,x\subset\mathcal{X}}$	0.37	0.27

2) Decomposing GP Regression Estimate: Fig. 6 shows a decomposition of the interaction effects with the highest impact on the resulting estimate, previously shown in Table II. It can be seen that the dominant interaction effect changes among the combination of learning inputs along the rover's trajectory. For example, $(\phi,q_1)_{rigid}$ and $(\phi,\theta,q_1)_{rigid}$ are the dominant interaction effects from 10 to $12m$, whereas $((\phi,\theta)_{rigid},speed)$ is the dominant interaction effect between 12 and $14.5m$.

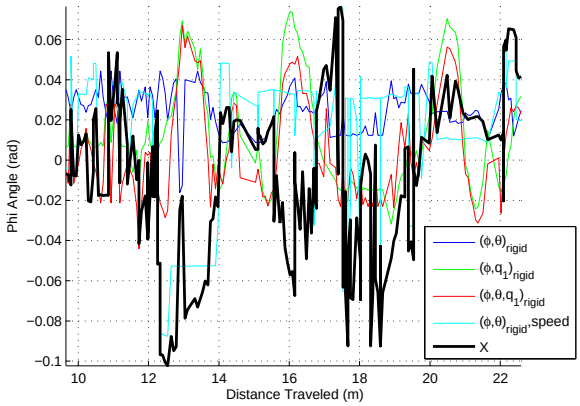

(a)

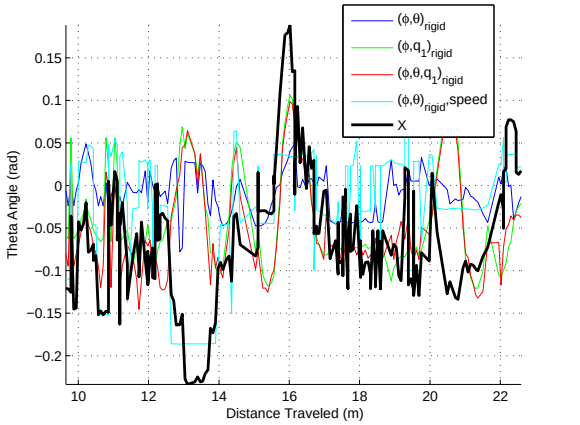

(b)

Fig. 6. Decomposition of interaction effects on rover roll ϕ (a), and pitch θ (b). The overall effect from all learning inputs X on the estimate of ϕ and θ is shown as the black line. The blue and green lines show the second order interaction effects from the learning inputs $(\phi, \theta)_{rigid}$ and $(\phi, q_1)_{rigid}$ respectively on the estimate. The impact of the third order interaction effects from the learning inputs $(\phi, \theta)_{rigid}, speed$ (teal) on the estimate can be seen particularly between 12 and $14m$ along its traveled distance where there is significant terrain deformation.

VI. Conclusion

In this paper, we analyzed the impact of learning inputs on a near-to-far terrain traversability estimation process, proposed by the authors in prior work, using a sensitivity analysis method built on Analysis of Variance (ANOVA) decomposition. The approach first decomposes the resultant estimate into a multi-dimensional representation of primary and interaction effects between the learning inputs, and then calculates the analytical sensitivity measure that indicates the significance of each learning input. We demonstrated the approach to assess the impact of terrain geometry and driving speed on the estimate of the rover's attitude and chassis configuration that accounts for the effects of terrain deformation. We showed that terrain geometry expressed as the rover's attitude and chassis configuration is the most informative among the learning inputs, having the highest analytical sensitivity measure as a primary effect. It was also significant as an interaction effect on the resulting estimate, when combined with driving speed. In future work, we will analyze the impact of additional modes of exteroceptive sensor data, such as terrain color and texture, using this analytical framework.

References

[1] J. Grant, A. Steele, M. Richardson, S. Bougher, B. Banerdt, L. Borg, J. Gruener, and J. Heldmann, "Mars science goals, objectives, investigations, and priorities: 2006," MEPAG, Tech. Rep., 2006.

[2] K. Iagnemma, S. Kang, H. Shibly, and S. Dubowsky, "Online terrain parameter estimation for wheeled mobile robots with application to planetary rovers," *IEEE Transactions on Robotics*, vol. 20, no. 5, pp. 921–927, 2004.

[3] A. Howard, M. Turmon, L. Matthies, B. Tang, A. Angelova, and E. Mjolsness, "Towards learned traversability for robot navigation: From underfoot to the far field," *Journal of Field Robotics*, vol. 23, no. 11-12, pp. 1005–1017, 2006.

[4] C. A. Brooks and K. Iagnemma, "Self-supervised terrain classification for planetary surface exploration rovers," *Journal of Field Robotics, Special Issue on Space Robotics, Part I*, vol. 29, no. 3, pp. 445–468, 2012.

[5] A. Krebs, C. Pradalier, and R. Siegwart, "Adaptive rover behaviour based on online empirical evaluation: Rover-terrain interaction and near-to-far learning," *Journal for Field Robotics*, vol. 27, no. 2, pp. 158–18 023, 2010.

[6] T. P. Setterfield and A. Ellery, "Terrain response estimation using an instrumented rocker-bogie mobility system," *IEEE Transactions on Robotics*, vol. 29, no. 1, pp. 172–188, 2013.

[7] D. R. Jones, M. Schonlau, and W. J. Welch, "Efficient global optimization of expensive black-box functions," *Journal of Global optimization*, vol. 13, no. 4, pp. 455–492, 1998.

[8] A. Saltelli, K. Chan, E. M. Scott, *et al.*, *Sensitivity analysis*. Wiley New York, 2000, vol. 134.

[9] I. M. Sobol, "On sensitivity estimation for nonlinear mathematical models," *Matematicheskoe Modelirovanie*, vol. 2, no. 1, pp. 112–118, 1990.

[10] M. Schonlau and W. J. Welch, "Screening the input variables to a computer model via analysis of variance and visualization," in *Screening*, A. Dean and S. Lewis, Eds. Springer New York, 2006, pp. 308–327.

[11] M. J. Bayarri, J. O. Berger, R. Paulo, J. Sacks, J. A. Cafeo, J. Cavendish, C.-H. Lin, and J. Tu, "A framework for validation of computer models," *Technometrics*, vol. 49, no. 2, 2007.

[12] T. A. Mara and S. Tarantola, "Variance-based sensitivity indices for models with dependent inputs," *Reliability Engineering & System Safety*, vol. 107, pp. 115–121, 2012.

[13] C. Xu and G. Z. Gertner, "Uncertainty and sensitivity analysis for models with correlated parameters," *Reliability Engineering & System Safety*, vol. 93, no. 10, pp. 1563–1573, 2008.

[14] G. Li, H. Rabitz, P. E. Yelvington, O. O. Oluwole, F. Bacon, C. E. Kolb, and J. Schoendorf, "Global sensitivity analysis for systems with independent and/or correlated inputs," *The Journal of Physical Chemistry A*, vol. 114, no. 19, pp. 6022–6032, 2010.

[15] G. M. Dancik and K. S. Dorman, "statistical analysis for computer models of biological systems using r." 2008, pp. 1966–1967.

[16] K. Ho, T. Peynot, and S. Sukkarieh, "A near-to-far non-parametric learning approach for estimating traversability in deformable terrain," in *Proceedings of the IEEE/RSJ International Conference on Robotics and Intelligent Systems*, 2013.

[17] ——, "Traversability estimation for a planetary rover via experimental kernel learning in a gaussian process framework," in *Proceedings of the IEEE International Conference on Robotics and Automation*, 2013.

[18] C. E. Rasmussen and C. K. I. Williams, *Gaussian Processes for Machine Learning*. Cambridge, MA: The MIT Press, 2006.

[19] R. Caruana, "Multitask learning," *Machine learning*, vol. 28, no. 1, pp. 41–75, 1997.

[20] G. Chastaing and L. L. Gratiet, "Anova decomposition of conditional gaussian processes for sensitivity analysis with dependent inputs," *arXiv:1310.3578*, 2013.

[21] J. P. Underwood, A. Hill, T. Peynot, and S. J. Scheding, "Error modeling and calibration of exteroceptive sensors for accurate mapping applications," *Journal of Field Robotics*, vol. 27, no. 1, pp. 2–20, 2010.